Bulletin of the Seismological Society of America

This copy is for distribution only by
the authors of the article and their institutions
in accordance with the Open Access Policy of the
Seismological Society of America.

For more information see the publications section
of the SSA website at www.seismosoc.org

THE SEISMOLOGICAL SOCIETY OF AMERICA
400 Evelyn Ave., Suite 201
Albany, CA 94706-1375
(510) 525-5474; FAX (510) 525-7204
www.seismosoc.org

Bulletin of the Seismological Society of America, Vol. 100, No. 4, pp. 1710–1723, August 2010, doi: 10.1785/0120080306

High-Resolution Seismic Reflection Imaging of Growth Folding and Shallow Faults beneath the Southern Puget Lowland, Washington State

by Curtis R. Clement,* Thomas L. Pratt, Mark L. Holmes, and Brian L. Sherrod

Abstract Marine seismic reflection data from southern Puget Sound, Washington, were collected to investigate the nature of shallow structures associated with the Tacoma fault zone and the Olympia structure. Growth folding and probable Holocene surface deformation were imaged within the Tacoma fault zone beneath Case and Carr Inlets. Shallow faults near potential field anomalies associated with the Olympia structure were imaged beneath Budd and Eld Inlets. Beneath Case Inlet, the Tacoma fault zone includes an ~350-m wide section of south-dipping strata forming the upper part of a fold (kink band) coincident with the southern edge of an uplifted shoreline terrace. An ~2 m change in the depth of the water bottom, onlapping postglacial sediments, and increasing stratal dips with increasing depth are consistent with late Pleistocene to Holocene postglacial growth folding above a blind fault. Geologic data across a topographic lineament on nearby land indicate recent uplift of late Holocene age. Profiles acquired in Carr Inlet 10 km to the east of Case Inlet showed late Pleistocene or Holocene faulting at one location with ~3 to 4 m of vertical displacement, south side up. North of this fault the data show several other disruptions and reflector terminations that could mark faults within the broad Tacoma fault zone. Seismic reflection profiles across part of the Olympia structure beneath southern Puget Sound show two apparent faults about 160 m apart having 1 to 2 m of displacement of subhorizontal bedding. Directly beneath one of these faults, a dipping reflector that may mark the base of a glacial channel shows the opposite sense of throw, suggesting strike-slip motion. Deeper seismic reflection profiles show disrupted strata beneath these faults but little apparent vertical offset, consistent with strike-slip faulting. These faults and folds indicate that the Tacoma fault and Olympia structure include active structures with probable postglacial motion.

Introduction

Shallow, active faults pose a seismic hazard to the ~3.3 million people living in the Puget Lowland of northwest Washington State. Northeast-directed subduction of the Juan de Fuca plate and northward motion of the Oregon Coast Range block have caused a series of faults and folds beneath the Puget Lowland (Pratt *et al.*, 1997; Wells *et al.*, 1998; Brocher *et al.*, 2001; Johnson *et al.*, 2004; Liberty and Pratt, 2008; Kelsey *et al.*, 2008). Pre-Quaternary strata beneath the Puget Lowland are largely covered by glacial deposits, the most recent being those of the Vashon stade of the Frasier glaciation that culminated about 16,400 years ago (Thorson, 1980; Booth, 1994; Porter and Swanson, 1998; Booth *et al.*, 2004). These glacial deposits mask older structures, but potentially record late Pleistocene and Holocene faulting, landsliding, and ice-meltout. We collected shallow, high-resolution marine seismic reflection profiles across the two potentially active faults, the Tacoma fault zone and the Olympia structure, which bound the north and south edges of the Tacoma basin. The purpose of this article was to determine whether faults or folds deform the shallow strata and to relate paleoseismic observations on nearby land to deeper structures. We also reexamined data from a trench across the Tacoma fault scarp to compare folding observed in the trench to that seen on the nearby marine seismic profiles. The seismic profiles image a growth fold within the upper 30 m of the Tacoma fault zone, with apparent vertical displacement of the water bottom that shows similarity to the folding in the trench. Possible postglacial faults were also

*Now at Earth Spring Energy, LLC, 1117 Maddox Creek Lane, Mount Vernon, Washington 98274, Curtis@earthspringenergy.com.

observed cutting shallow strata along parts of the central Tacoma fault zone and the Olympia structure. The results thus document recent folding or faulting on both the north and south edges of the Tacoma basin.

Previous Work

Deformation in the Puget Lowland region has formed a series of fault-bounded or fold-bounded basins and uplifts (Gower *et al.*, 1985; Pratt *et al.*, 1997; Brocher *et al.*, 2001). The density contrast between the sediment-filled basins and the areas of uplifted Crescent Formation volcanic basement rocks cause prominent gravity and magnetic anomalies that delineate west or northwest-trending faults and folds, such as the southern Whidbey Island fault (SWIF), Kingston Arch, Seattle fault, Tacoma fault, and Olympia structure (Fig. 1; Gower *et al.*, 1985; Finn, 1990; Finn *et al.*, 1991; Johnson *et al.*, 1994; Pratt *et al.*, 1997; Brocher *et al.*, 2001; ten Brink *et al.*, 2002; Blakely *et al.*, 2002; Johnson *et al.*, 2004; Sherrod *et al.*, 2008; Liberty and Pratt, 2008; Kelsey *et al.*, 2008). These structures beneath the Puget Lowland are hypothesized to be part of an interconnected system accommodating the north to northeast compression in the area (Pratt *et al.*, 1997; ten Brink *et al.*, 2002; Brocher *et al.*, 2004; Johnson *et al.*, 2004).

Although an M 7+ earthquake was documented to have ruptured the Seattle fault in the central Puget Lowland about 1100 years ago (Bucknam *et al.*, 1992; Nelson *et al.*, 2003), the Tacoma fault and Olympia structure have received less attention. On the north edge of the Tacoma basin, geophysical data show a west-trending series of faults and folds interpreted to be a broad Tacoma fault zone (Pratt *et al.*, 1997; Brocher *et al.*, 2001; Johnson *et al.*, 2004). Pratt *et al.* (1997) interpreted the central part of the Tacoma fault zone as a south-dipping monoclinal fold or ramp, later termed the Rosedale monocline (Fig. 2a) by Johnson *et al.* (2004), but tomographic models to the west suggest the Tacoma structure is a north-dipping reverse fault there (Brocher *et al.*, 2001). Johnson *et al.* (2004) interpreted the Tacoma fault zone as an east-trending fault that crosses the Lowland, intersecting the northwest-trending Rosedale monocline beneath the central and east Lowland (Fig. 2a). Seismic reflection profiles across the western part of the Tacoma fault zone beneath Case Inlet show a 360-m wide kink band that appears to be a growth fold above a deeper fault (Johnson *et al.*, 2004).

The Olympia structure at the south edge of the Tacoma basin (Fig. 1) remains enigmatic because the shallow inlets of southern Puget Sound prevent the collection of deep-penetration marine seismic reflection profiles across it (Pratt *et al.*, 1997). The Olympia structure separates the 3.5 to 6.0 km of sedimentary strata in the Tacoma basin from uplifted Crescent Formation basement rocks exposed in the Black Hills south of the Lowland (Pratt *et al.*, 1997; Brocher *et al.*, 2001). Coincident gravity and magnetic gradients show the structure to be approximately 80 km long with a trend of about 315° (Fig. 1; Finn, 1990; Finn *et al.*, 1991; Blakely *et al.*, 1999). The linearity of the potential field anomalies suggests that the Olympia structure is a fold or fault. Industry seismic reflection data at the northeast edge of the Olympia structure show a gently north-dipping reflector, interpreted as the top of Crescent Formation basement rocks, overlain by nearly flat sedimentary strata of the Tacoma basin (Pratt *et al.*, 1997). The southern portion of the Olympia structure, with the most prominent potential field anomalies, has not yet been imaged on deep-penetration seismic profiles. Pratt *et al.* (1997) proposed that the Olympia structure is a ramp above the base of a fault, but this interpretation is not compelling because reflector onlap suggests that the Tertiary strata in the southern Tacoma basin were deposited on a sloping surface with only slight folding (2° to 4° tilt) after deposition. Alternatively, the Olympia structure could be a predominantly pre-Tertiary fold that is cut by a fault south of the existing industry seismic profiles.

Evidence for Holocene land-level changes along the Tacoma fault and Olympia structure suggest that there was a large earthquake about 1100 years ago in the southern Puget Lowland (Bucknam *et al.*, 1992; Sherrod, 2001). Sherrod *et al.* (2004) document an uplifted tidal flat (terrace) at Case Inlet and a series of east-trending, south-facing, *en echelon* topographic lineaments deforming the late Pleistocene to Holocene glacial deposits along the west part of the Tacoma fault zone (Fig. 2b). The lineaments are ~80-m wide sloping surfaces that form scarplike linear features that we will refer to as fold scarps. A trench dug across one of these lineaments, the Catfish Lake fold scarp, showed a fold in the strata with more than 2 m of vertical relief, up to the north, but only minor faulting (< 30 cm; Sherrod *et al.*, 2003, 2004). Their interpretation of the trench exposure is that the fold scarp is caused by warping of the postglacial surface above a blind fault tip. Late Quaternary motion has not been convincingly documented on structures forming the central and eastern portions of the Tacoma fault zone, although Johnson *et al.* (2004) compiled evidence consistent with recent motion. Subsidence of marshes also occurred in southernmost Puget Sound about 1100 years ago, consistent with motion on a fault or fold near Olympia (Sherrod, 2001).

Data Acquisition

We collected single-channel marine seismic reflection profiles using a sparker seismic source towed behind the University of Washington's R/V *WeeLander*. The waterways in Puget Sound are nearly perpendicular to the major geophysical anomalies, so the main profiles were acquired along the shores or down the centers of the inlets.

During acquisition, we fired the 300-joule minisparker source every 0.5 sec with a vessel speed of about 6 km/hr. Single-channel seismic reflection data were collected using a 10-m long hydrophone streamer. Digital data were recorded at 4000 samples/sec using a PC-based acquisition system (U.S. Geological Survey's Mudseis system). Record length was set at 0.25 sec, resulting in approximately 200 m

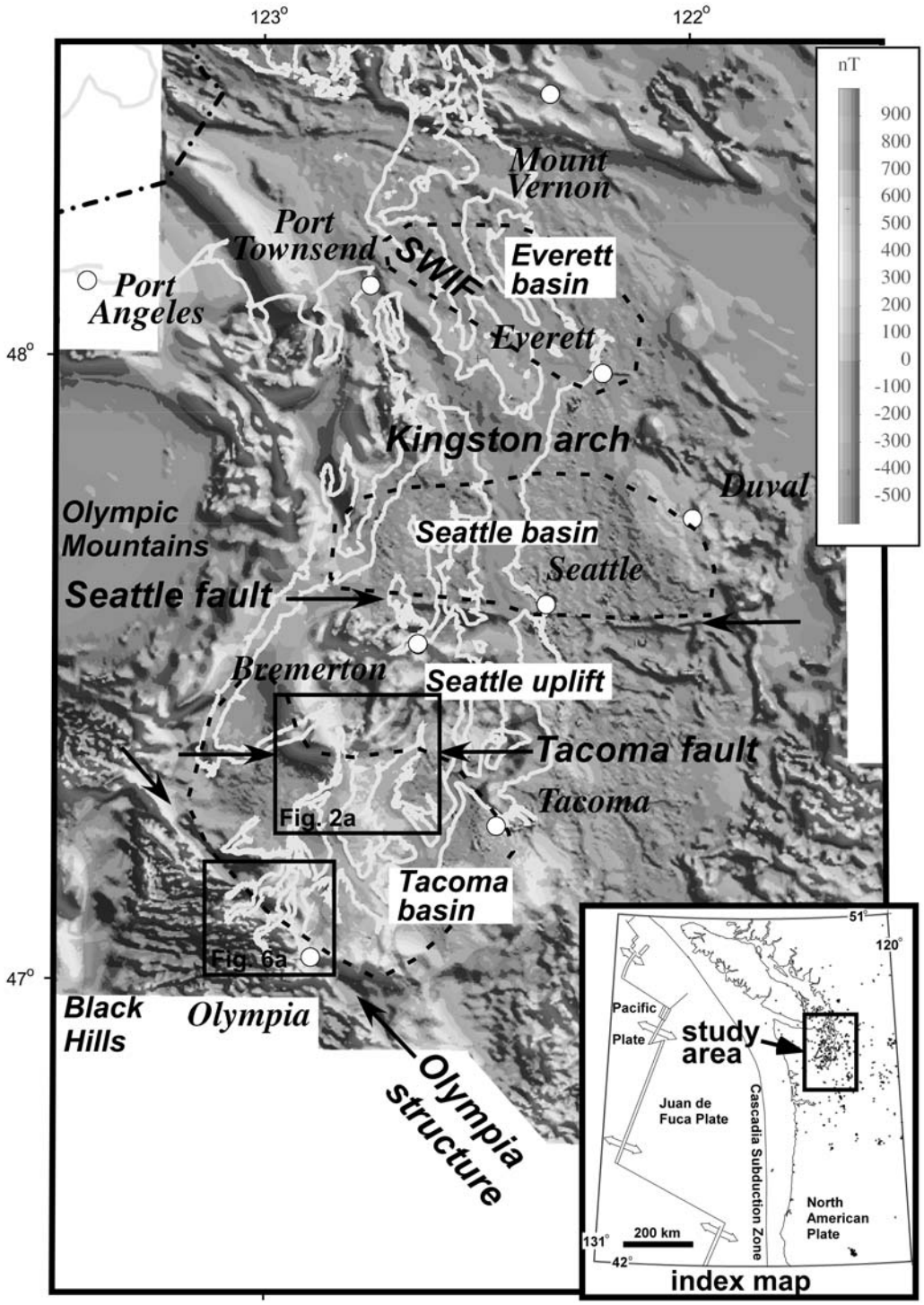

Figure 1. Magnetic map from Blakely *et al.* (1999) showing the major faults and folds beneath the Puget Lowland (black arrows). The black rectangles show the Tacoma and Olympia study light detection and ranging (LiDAR) maps shown in Figures 2a and 6a, respectively. Heavy dashed lines outline the Tacoma, Seattle, and Everett basins, as determined by the 4.25 km/sec contour on a tomography image at 2.5 km depth (Van Wagoner *et al.*, 2002). SWIF: Southern Whidbey Island fault.

maximum depth of penetration, but no reflectors were imaged at depths below about 150 m. Significant pockets of gas have accumulated within the sediments of these shallow waterways due to high organic content; as a result, sub-bottom penetration was blocked along large stretches of some profiles.

The data were band-pass filtered (300–1200 Hz), deconvolved, and migrated. Migrations utilized a Stolt f-k algorithm assuming a constant velocity of 1500 m/sec, as single-channel data do not provide accurate velocity information. The vessel's position was recorded at 5-sec intervals

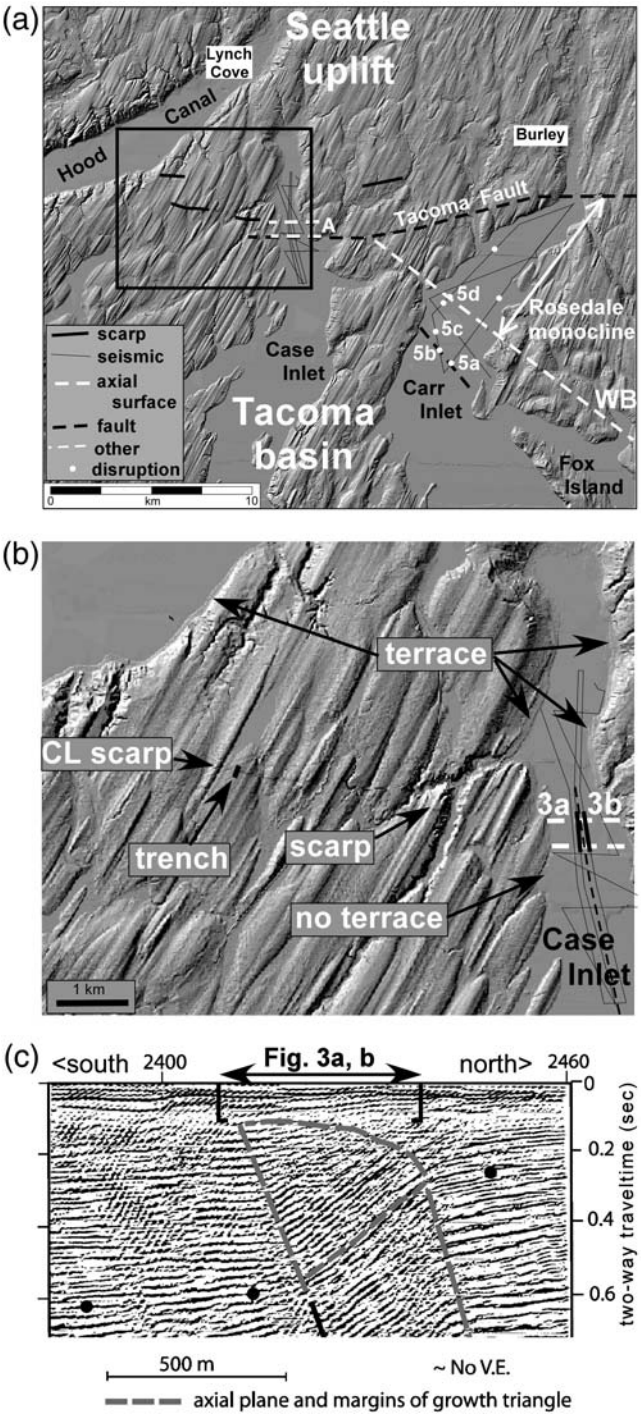

Figure 2. (a,b) LiDAR maps (Haugerud *et al.*, 2003) of the Tacoma fault zone showing the Catfish Lake fold scarps (CL scarp) and trench west of Case Inlet, the location of the kink band (white dashed lines labeled A) imaged on seismic reflection data (Johnson *et al.*, 2004), the terrace surrounding the north end of the inlet, and the track lines for our seismic reflection profiles (thin black lines). Numbers and letters indicate figure numbers that show the indicated features. Location of the Rosedale monocline is from Johnson *et al.* (2004). WB: Wollochet Bay. (c) Seismic reflection profile from Johnson *et al.* (2004) showing kink band beneath Case Inlet. Black dots show interpreted base of Quaternary strata. The portion of the profile shown here is the north part of the dashed black line in Figure 2b where the profile crosses the kink band (white dashed lines).

using differential GPS, giving an estimated location precision of about 6 m. This same seismic system, with a comparable source, was effective at imaging shallow strata in other seismically active regions (e.g., Pratt *et al.*, 2001, 2003).

Growth Folding within the Western Tacoma Fault Zone

Our data across the western Tacoma fault in Case Inlet imaged gentle folding, a warped water bottom, and strata indicative of growth folding above a blind thrust or reverse fault. Johnson *et al.* (2004) document south-dipping strata in a 360-m wide kink band beneath Case Inlet on seismic reflection data acquired with a small airgun (Fig. 2c). Our profiles image the kink band as a panel of south-dipping strata, with dips increasing downward to create a fanning sequence (Fig. 3a,b). The panel has a width of about 350 m on our profiles, but the south end is obscured by the onset of a strong reflector that is probably a gas-saturated layer near the water bottom. The north edge of the kink band is marked by a change from dipping to horizontal strata, as on the airgun profile. Dips within the kink band increase downward to about 5° at a depth of about 40 m (dipping reflector in Fig. 3a,b). Johnson *et al.* (2004) show that the dips continue to increase to about 35° dip at and below 300 m depth (~0.4 sec traveltime; Fig. 2c). The deeper profile is consistent with a fault extending to as shallow as 200 m depth (0.25 sec; Johnson *et al.*, 2004). We propose that the shallow strata we imaged were deformed by growth folding and minor faulting above this active fault tip.

The water bottom is warped upward about 2 m above the center of the kink band (Fig. 3a,b), suggesting Holocene fold growth. The warping forms a distinct, ~100-m wide sloping surface on the water bottom. We interpret this slope as a fold scarp forming the southern edge of the uplifted terrace and tidal flat that lies north of the kink band, and to be the underwater extension of the *en echelon* fold scarps visible on light detection and ranging (LiDAR) data to the west (Fig. 2b).

The pattern of folding within the shallow strata beneath Case Inlet suggests that the kink band is a growth fold that was initiated in the Quaternary. Horizontal strata in the upper 5 m onlap slightly south-dipping, postglacial sediment layers deeper in the kink band (Fig. 3a). The postglacial strata beneath the onlapping sequence exhibit about 5 m of vertical change across the fold. A deeper, probably late Pleistocene reflector has a dip of about 5° on our profiles and shows vertical relief of about 20 m across the kink band (dipping reflector in Fig. 3a,b). Upper Quaternary strata show the shallow fanning sequence, but deeper strata within the kink band appear to be parallel and therefore predate the folding (Fig. 2c; Johnson *et al.*, 2004). The warping of the water bottom seen on the seismic reflection profile is similar in amplitude and wavelength to that at the Catfish Lake fold scarp to the west (Sherrod *et al.*, 2003, 2004), and it lies at the south edge of the uplifted terrace. The data therefore are consistent with latest

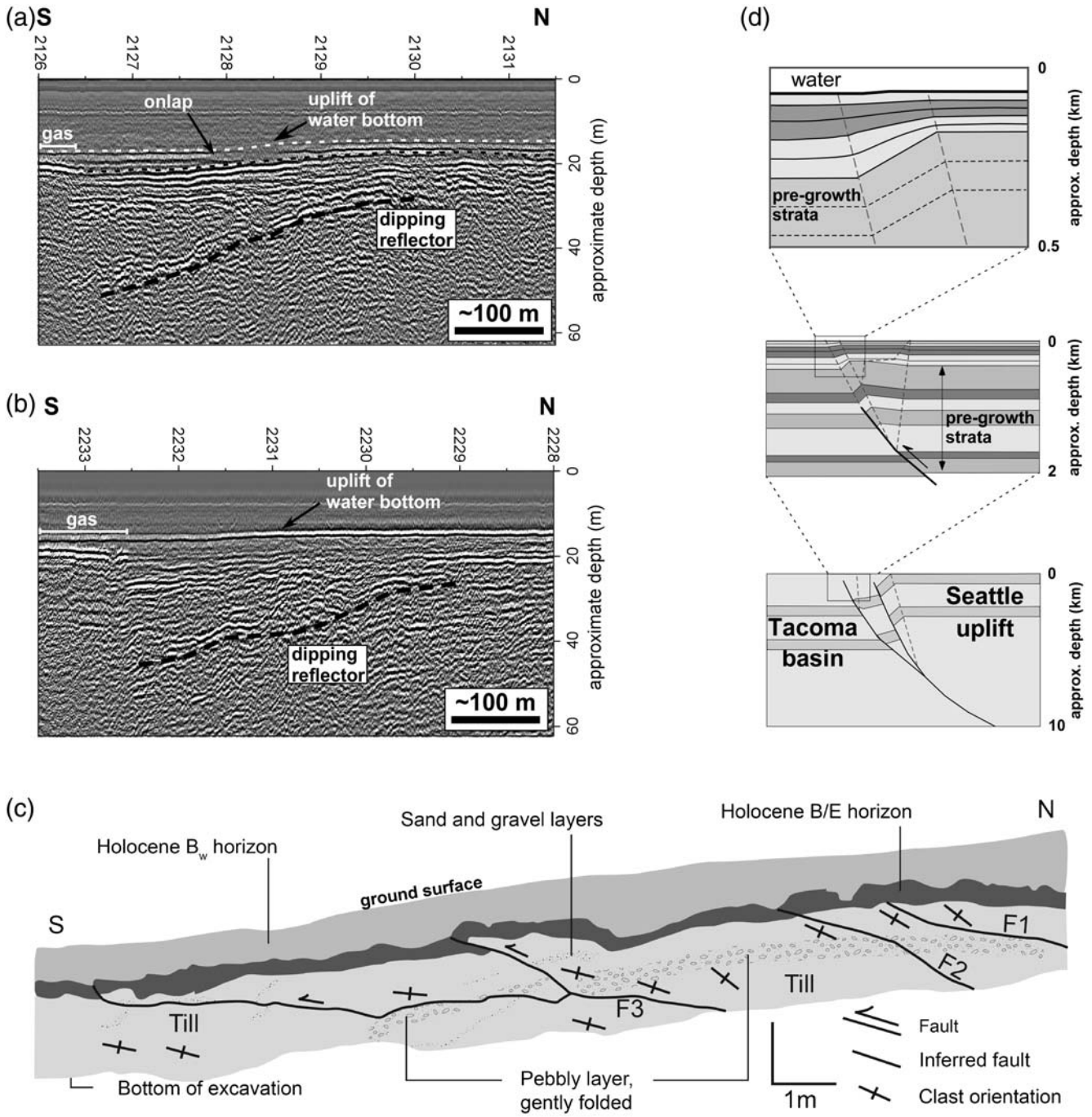

Figure 3. Growth folding at Case Inlet (Fig. 2a,b) and at the trench west of the inlet. (a,b) Parallel seismic reflection profiles (see Fig. 2 for location) showing growth folding, onlap of shallow strata, and warped water bottom at the top of the kink band. Dashed lines lie just below the dipping reflectors mentioned in the text. (c) Central 17 m of the trench log from Sherrod *et al.* (2003, 2004) showing the folding and minor faulting (F1, F2, and F3) discussed in the text. Location of trench is shown in Figure 2b. The fold scarp is about 50- to 60-m wide. (d) Kinematic model showing the kink band to be growth folding above a buried fault.

Pleistocene or Holocene growth of the kink band in response to motion on an underlying fault (Fig. 3d).

Growth folding within the kink band beneath Case Inlet is consistent with geomorphic and paleoseismic observations made on the Catfish Lake fold scarp immediately to the west (Sherrod *et al.*, 2003, 2004). A 30-m long trench across the fold scarp (Fig. 2b) exposed late Quaternary glacial sediments (till, sand, and gravel-filled channels), deposited by the last glacial ice sheets (Booth, 1994). The oldest unit exposed in the excavation was a dense sandy silt with abundant faceted gravel and cobbles (Fig. 3c). Clasts in the dense silt were imbricated in many places and displayed a crude stratification. The density, heterogeneity, and abundance of faceted clasts suggest that this deposit is a lodgement till. The deepest

excavated soil horizon, which lies directly on the till surface, is a gray silty B/E horizon with platy structure. Immediately overlying the B/E horizon is a weakly developed B horizon (B_W), consisting of pale brown loamy sand to sandy loam. The uppermost horizon (A horizon) consists of dark brown lenses of organic material.

Deposits in the excavation showed evidence of postglacial folding and minor faulting (Sherrod *et al.*, 2003, 2004). Deformation observed in the till is consistent with both glacial ice flow and movement on the Tacoma fault. Folding of till fabrics is defined by stratified pebbles and imbricated clasts. Pebble layers in the north half of the trench are almost horizontal, whereas similar layers in the southern half of the trench dip to the south. Imbricated clasts are more steeply inclined on the north side of fault F3 (Fig. 3c) and are almost subhorizontal to the south of F3. The break between the two fabric orientations occurs near F3, and both fabrics suggest anticlinal folding. However, the platy B/E horizon of the surface soil is displaced by F3 with ~30 cm of reverse offset. No organic material suitable for radiocarbon dating was present. Folded and faulted glacial deposits show that most of the deformation and scarp height postdate deposition by the ice sheet, which ended in this area about 16,400 years ago (Porter and Swanson, 1998).

The fold scarps beneath and west of Case Inlet coincide with the south edge of shorelines that were uplifted in an earthquake between A.D. 770 and 1160 (Sherrod *et al.*, 2004). A raised tidal flat observed along the shores of Case Inlet north of the kink band indicates 4 m of late Holocene uplift (Fig. 2b). Raised tidal flat deposits north of the fault contain marine fossils. Paleoecology of the tidal flat deposits and overlying upland soils require at least 1.5 m of uplift to change a tidal flat into a freshwater swamp or meadow (Bucknam *et al.*, 1992; Sherrod, 2001). Ages of plant fossils within the tidal flat deposits and from overlying freshwater peat limit uplift to between A.D. 770 and 1160 (Sherrod *et al.*, 2004).

Radiocarbon ages from other uplifted or submerged coastal sites straddling the Tacoma fault also constrain the timing of a deformation event to between A.D. 770 and 1160. An age from leaf bases of *Triglochin maritima* that grew on a freshly uplifted tidal flat surface at Lynch Cove (Fig. 2a) constrain uplift to shortly before A.D. 880–980. Similarly, freshwater peat deposited between A.D. 1000 and 770 at Burley (Fig. 2a) overlies sand vented onto a raised tidal flat, implying that the ground shook hard enough to liquefy during uplift. At other sites, ages on freshwater swamp peat deposited over tidal flat deposits loosely constrain uplift between A.D. 890 and 1410. A single age from a submerged tree south of the Tacoma fault constrains subsidence to between A.D. 980 and 1190. Sherrod (2001) and Sherrod *et al.* (2000, 2004) also document coseismic submergence south of the Tacoma fault at Wollochet Bay (Fig. 2a) between 1010 and 1150 years ago.

Other features on the Case Inlet seismic profiles have northeast trends that are approximately parallel to the glacial lineations (Fig. 4a) and are likely glacial in origin, although we cannot eliminate tectonic origins. One such feature is an ~300-m wide ridge that appears to be onlapped by postglacial sediments (Fig. 4b). On one profile this ridge is completely covered by undisturbed sediments, but on others its top is exposed, and it has slight depressions on its edges. One interpretation is that this ridge formed by faulting, perhaps being the forelimb of a fault-propagation fold or a pop-up (flower) structure between two faults, with deformation releasing the gas from the overlying muds. However, a glacial origin is suggested by the strike of the feature being approximately parallel to the glacial lineations, at a high angle to the known fault scarps and geophysical anomalies (Fig. 4a). One possibility is that it is glacially carved, as were the ridges on the surrounding land areas, with tidal currents scouring slight depressions on its margins and keeping the young sediments clear of gas by preventing the accumulation of fine sediments.

A second feature obvious on the profiles is a change in water depth at the entrance to the northernmost arm of Case Inlet (Fig. 4c). This bathymetric step has a northeast trend that is approximately parallel to glacial features (ridges and troughs) on the surrounding land. Again the step could be tectonic in origin, but the strike is at a high angle to the Tacoma fault and the geophysical anomalies, and does not coincide with the southern limit of the uplifted terrace. A simpler explanation is that the inlet is shallower toward its head; this decrease occurs in steps that are controlled in part by the glacial ridges.

Shallow Faults beneath Carr Inlet in the Central Tacoma Fault Zone

Our Carr Inlet seismic profiles across the central Tacoma fault zone image strata that we interpret as Pleistocene glacial deposits covered by up to 20 m of late Pleistocene and Holocene postglacial sediments. The contact between these two units is a strong reflector that we interpret as an erosional unconformity, with the inferred Pleistocene glacial deposits beneath the unconformity having a hummocky appearance with discontinuous reflectors (Fig. 5b). Profiles perpendicular to the shorelines show the upper surface of these glacial deposits sloping gently toward the middle of the inlet, with the overlying subhorizontally stratified sediments onlapping this sloping surface. The late Pleistocene and Holocene sediments show slight folding or draping over the Pleistocene erosional surface. In many areas, including most of the deeper parts of the inlet, there was little signal penetration through a strong reflector within the shallow sediments (left side of Fig. 5b). We interpret this strong reflector as a gas-saturated layer.

The Carr Inlet profiles show shallow, postglacial faulting near the Rosedale monocline (Fig. 5a) of Johnson *et al.* (2004). A probable fault, defined by abrupt changes in depth, by possible diffractions, and by folding of postglacial sediments (Fig. 5b), lies within the flat-lying Tacoma basin strata about 3 km southwest of the axial surface at the base of the monocline (Fig. 2a; Pratt *et al.*, 1997; Johnson *et al.*, 2004). The shallow fault shows 3 to 4 m of vertical displacement, south side up, on strata within the postglacial deposits, and

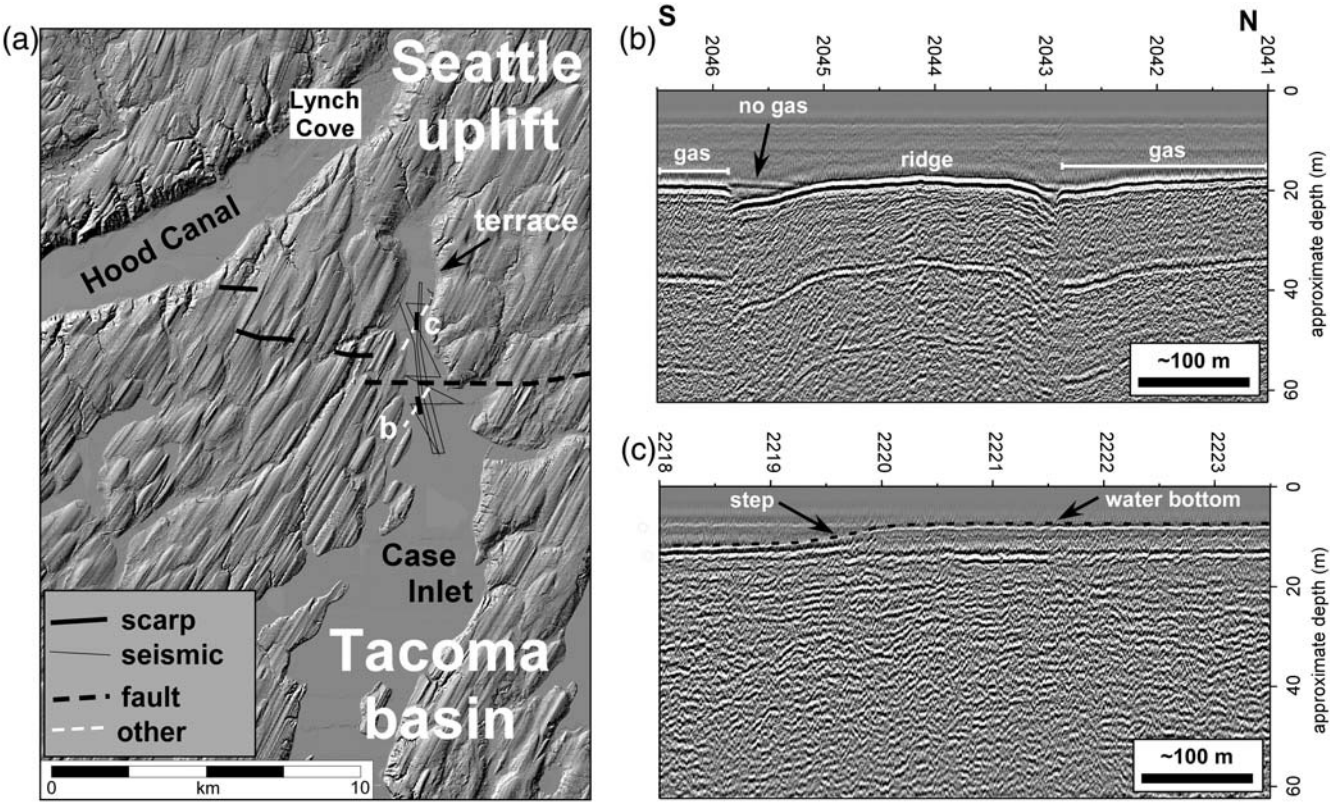

Figure 4. (a) LiDAR map of Case Inlet and surrounding region showing the locations of probable glacial features (white dashed lines b and c) visible on the seismic profiles and shown in (b) and (c). They are likely glacial in origin because their trends are nearly the same as the glacial lineations. Locations of profiles in (b) and (c) are shown as heavy lines in (a). The strong reflector in (b) that mimics the water bottom is a multiple reflection.

shows prominent diffractions that indicate truncations of strata (*A* on Fig. 5b). These diffractions were not entirely removed by migration, possibly because our estimated velocities are incorrect or the fault is oblique to the profile. The postglacial strata on the south side of the fault are arched upward, but the water bottom does not appear to be deformed. Reflectors within the underlying glacial deposits show only slight disruptions at the fault, although the reflectors are hummocky and discontinuous by nature. About 100 m to the south of the interpreted fault, diffractions and terminations of strong reflectors in the postglacial sediments could mark another fault coincident with the abrupt onset of a gas-saturated layer (Fig. 5b).

We cannot identify the fault with certainty on adjacent profiles, but two other potential faults are imaged to the northwest. One nearby feature is a disrupted area on the profile in which arching of the shallow layers is visible below a break in the strongly reflective, gas-saturated layer (Fig. 5c). One interpretation is that faulting caused the arching and released gas from the shallow layers; however, the disrupted area cannot clearly be attributed to a fault, nor can we eliminate the possibility that the two profiles are imaging different structures. Another set of late Pleistocene or Holocene faults may be imaged just north of the disrupted area (Figs. 2a, 5e). The possible faults are defined by steps, abrupt changes in dip, and changes of character in the strong unconformity reflector at the top of the glacial deposits. This reflector is flat and relatively featureless throughout most of the rest of the inlet. Reflectors are arched and abruptly change dip at the potential faults. There is also scattered energy that may be in part diffractions that are improperly migrated because we are crossing a fault obliquely. The water bottom does not appear to be disturbed above these faults, but we do not know the sedimentation rate (or erosion rate) to constrain the age.

If either of the latter features are the westward extension of the fault, it has a trend of about 320°, nearly parallel to the axial surface inferred from deeper seismic data and potential field data (Fig. 2a). A fault is not interpreted on deeper seismic reflection profiles (Pratt *et al.*, 1997; Johnson *et al.*, 2004), perhaps because the total vertical displacement is less than the minimum resolution of the industry data. The fault also has not been identified in LiDAR data on the adjacent land (Fig. 2a). Thus, we interpret at least one fault beneath Carr Inlet, but we cannot confidently relate it to nearby structures.

The axial surface at the base of the Rosedale monocline (Figs. 2a, 5a) coincides with a change in slope and a possible disruption of the late Pleistocene erosional surface, and with slight folding of the postglacial sediments (Fig. 5e).

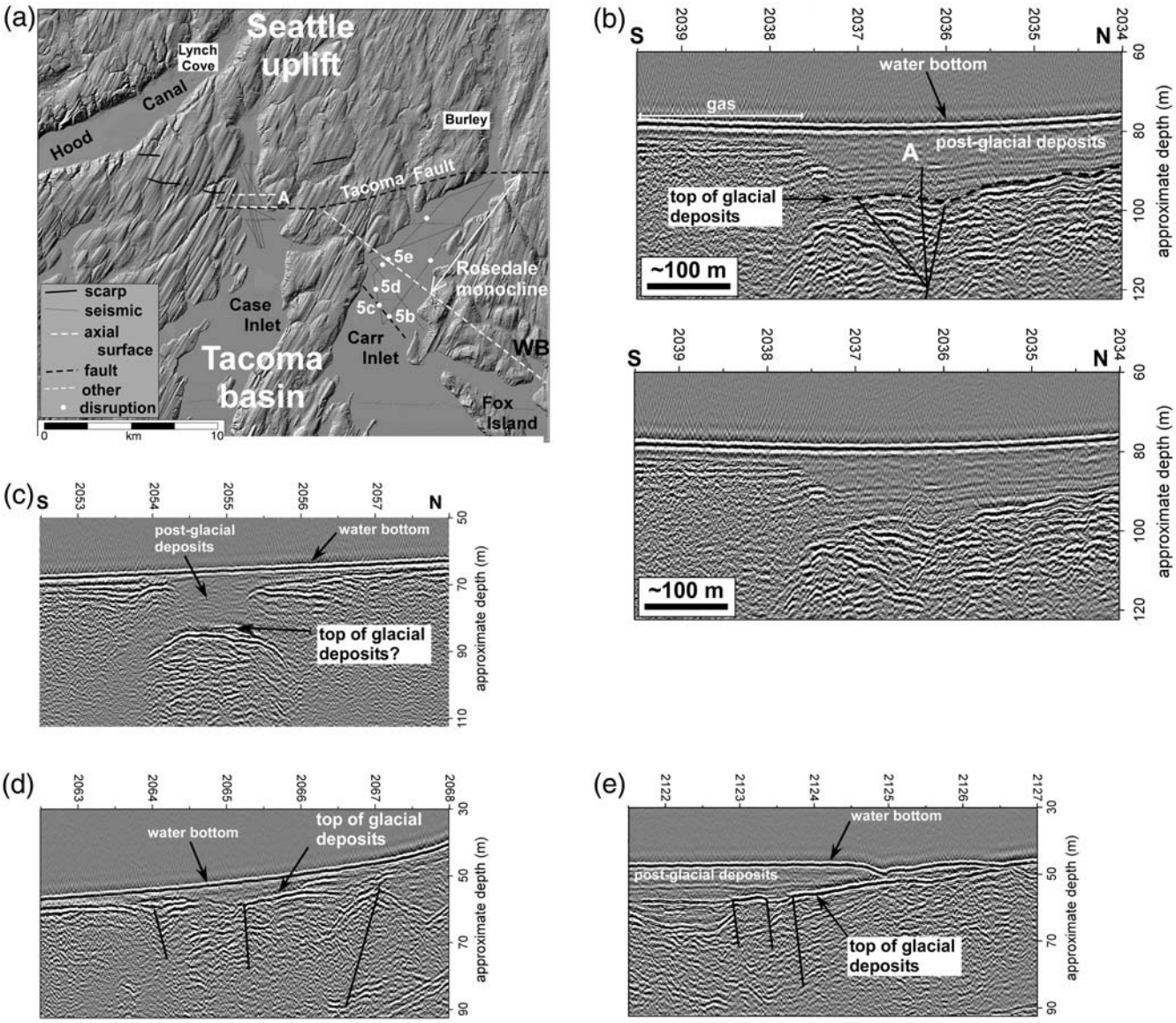

Figure 5. Shallow faults beneath Carr Inlet. (a) Location map with white dots showing disrupted zones. The locations of features shown in the other parts of the figure are labeled with the figure number. (b) Shallow fault that appears to cut postglacial strata (annotated and unannotated versions). (c) Disruption that allows signal penetration through the shallow, gas-saturated layer. A fault is one potential explanation for the disruption. (d) Apparent faults disrupting the unconformity at the base of postglacial deposits. (e) Apparent faults and change in dip of the unconformity at the axial surface of the Rosedale monocline.

The erosional unconformity is flat to the south of the axial surface, but is gently south-dipping to the north (2° dip; Fig. 5e). Coincident with the change in dip are three apparent faults that deform the postglacial sediments and break the erosional surface into small blocks (~60 m wide) that have been uplifted or downdropped 1 to 2 m. The change in dip of the erosional surface is suggestive of folding at the axial surface, but it could equally well be unrelated to tectonic activity. Specifically, the change in dip could be related to the sloping side of the channel, with our survey fortuitously crossing the slope break near the axial surface. The postglacial sediments onlap the dipping erosional surface (Fig. 5e), suggesting that the tilting predates the sediments. The disruptions in the late Pleistocene surface and the slight folding of the postglacial sediments suggest late Pleistocene or Holocene faulting.

Shallow Faulting and Folding within the Olympia Structure

Our seismic surveys across the Olympia structure provide images of apparent faults cutting subglacial or postglacial strata of late Pleistocene or Holocene age. Our profiles from Budd Inlet show small basins or channels up to 3.5 km wide and 140 m deep that are characterized by dipping reflectors at their base, which we interpret as erosional unconformities overlain by subhorizontally layered strata. Geologic maps

show the surrounding points of land to be pre-Vashon deposits (> 16, 400 years old) along the shorelines, overlain by Vashon till (Palmer *et al.*, 1999). Extensive, deep channels were cut into these pre-Vashon deposits beneath the glaciers (e.g., Booth, 1994; Booth *et al.*, 2004); many of these channels were filled with subglacial and unconsolidated recessional deposits as the glacier retreated about 16,400 years ago (Porter and Swanson, 1998).

Faults appear to cut the interpreted subglacial and recessional deposits imaged on our profiles across the Olympia structure. Our profile from the east side of Budd Inlet shows a channel feature defined by a north-dipping reflector (an erosional surface) beneath a horizontally layered sequence (Fig. 6c). Within the layered sequence, two faults appear to cut a 20-m thick packet of prominent reflectors between 50 and 70 m depth. The southern fault is expressed on our profile as a 10-m wide sag feature, with sedimentary strata on the north side lying 1 to 2 m deeper than equivalent strata to the south. The depression may be caused by minor extension or by compaction from dewatering within a fault zone. The fault may extend to within a few meters of the water bottom, where reflectors appear to be disrupted. The dipping reflector marking the unconformity at the base of the horizontal strata appears to be displaced 1 to 2 m with the opposite sense of motion (up to the north) than the overlying strata. The differing senses of displacement on reflectors of different depths indicate either strike-slip motion or reactivation of the fault with a different sense of displacement. We favor the strike-slip interpretation because we do not expect the stress regime to have changed significantly during the Quaternary.

Our eastern Budd Inlet profile shows what could be another fault with about 2 m of vertical displacement approximately 160 m to the north of the sag feature (Fig. 6c). This apparent fault appears as an ~20-m wide nonreflective zone, with the prominent layered sequence lying about 2 m deeper on the north side. Reflector truncations and a notch in the water bottom suggest recent motion may cut the shallowest strata.

On the west side of Budd Inlet, our seismic profile images what could be the westward extension of the sag feature associated with the southern fault on our eastern profile (Fig. 6d). Here the sag feature is clearly imaged extending into the shallowest strata just below the water bottom. The sagging is more pronounced than on the eastern profile, possibly indicating greater displacement or more extension on this part of the fault. A fault connecting the two sag features would have a strike of about 285°, which differs significantly from the 315° strike of the Olympia structure (Fig. 6a). However, the potential field anomalies show a variety of strike directions in the Black Hills (Fig. 1); this may indicate the presence of faults with several orientations. The northern fault on our eastern profile does not have an equivalent structure on the western profile (Fig. 6d), but a fault could pass through the nonreflective area on the western profile about 200 m north of the sag feature.

The sense of vertical displacement of the layered sequence on both of the faults beneath Budd Inlet, up to the south, is consistent with the long-term motion that down-dropped the Tacoma basin and brought Eocene Crescent Formation rocks to the surface in the Black Hills. We may be imaging multiple strands of a thrust or reverse fault, or *en echelon* strike-slip faults.

Topographic (LiDAR) data may show evidence for the faults we imaged on the seismic data, consistent with motion since the last glaciation ~16, 400 years ago (Thorson, 1980; Porter and Swanson, 1998). The trend of our interpreted fault through the sag feature extends near a faint lineament visible in LiDAR topographic data approximately 2 km to the west (Fig. 6a,b). This lineament shows only a slight elevation change and would not normally be identified as a fault scarp because of the lack of a vertical offset across it. Its main expression consists of stream valleys that appear to be aligned along it. However, the apparent faults in the seismic data have only 1 to 2 m of vertical displacement, and the predominant motion may be strike slip. A second, parallel lineament, also weakly expressed, lies about 1 km farther south. These topographic lineations are far more subdued than the fault scarps evident in LiDAR data near Case Inlet (e.g., Sherrod *et al.*, 2004; Fig. 2b), but their location along the projected trend of apparent faults suggests they could have a tectonic origin.

Deeper seismic reflection profiles suggest that the faults we imaged are part of a broader zone of deformation that also displaces deeper strata. In 1997 the USGS collected a series of seismic reflection profiles throughout southern Puget Sound using a small airgun source. The data were filtered and stacked and are available on a USGS website (U.S. Geological Survey, 2010). Portions of these profiles are presented in Johnson *et al.* (2004), but the profiles south of the Tacoma fault remain unpublished. We migrated the stacked seismic profiles from southernmost Puget Sound using a Stolt f-k algorithm and an estimated velocity function, as the hydrophone streamer was too short for accurate velocity determination.

The airgun profiles near the Olympia structure show gently north-dipping reflectors in the upper second (~1 km depth; Fig. 7). These strata are disrupted on all of the profiles near the mouths of Budd and Eld Inlets by an ~2-km wide zone of gently folded strata (Fig. 7). The faults imaged on our shallow sparker data lie within this zone of folded strata, suggesting that the shallow faults are controlled by deeper structures. Faults may also be evident from apparent reflector truncations within this disrupted zone. The most prominent of the deformation features is at the south edge of the zone, where strata are folded upward near what may be a fault. The apparent fault appears to be near-vertical and exhibits what may be a prominent step in the water bottom. This step in the water bottom appears to have a northwest trend if the same feature is being imaged just north of the 5 km marks on the two parallel profiles shown in Figure 7. The combination of gentle folds and near-vertical faults with small amounts of

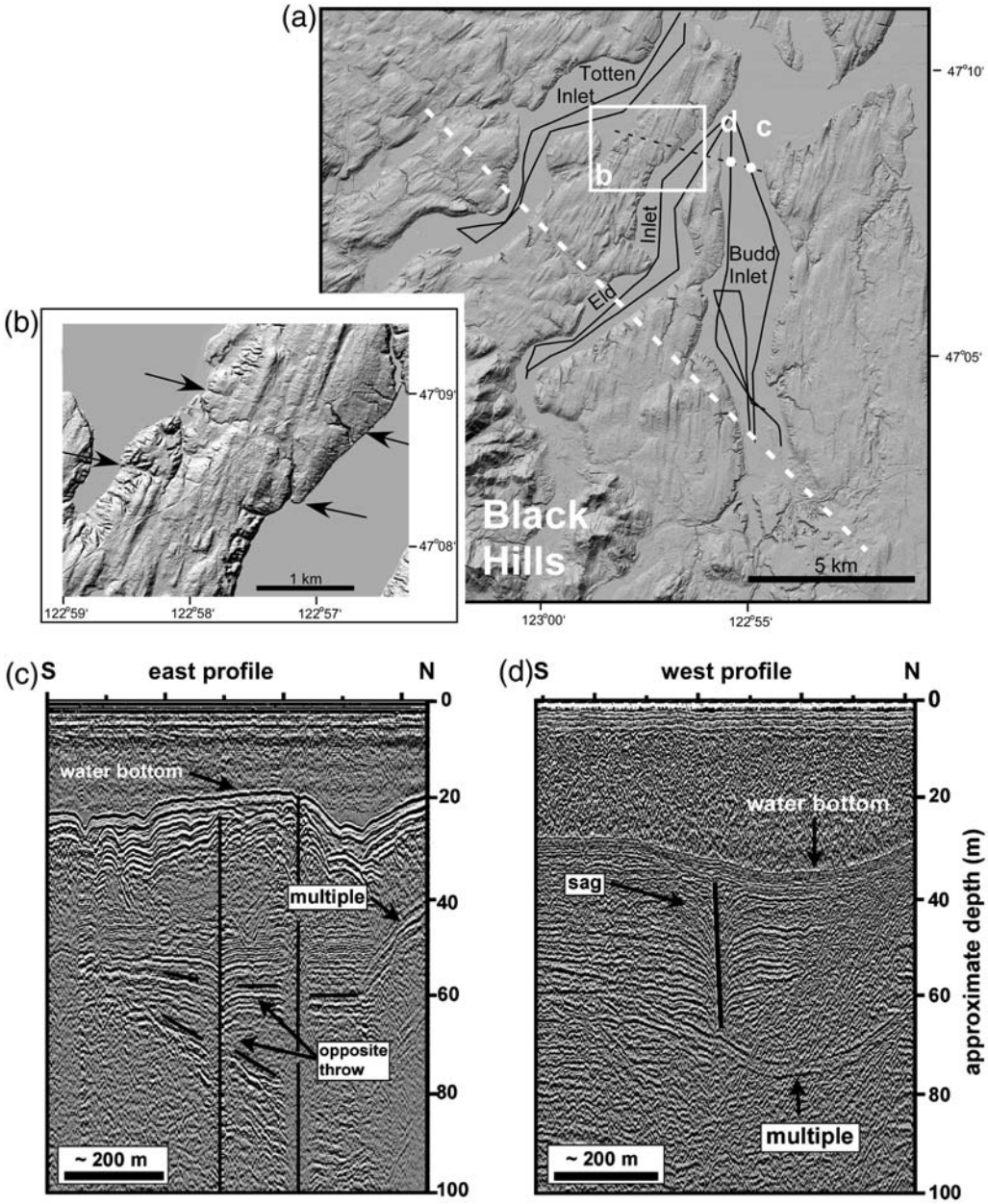

Figure 6. Shallow faults beneath Budd Inlet. (a) LiDAR map shows the locations of our seismic profiles in Budd, Totten, and Eld Inlets (black lines). White dashed line is the approximate location of the Olympia structure based on potential field data. White dots are the locations of faults shown on lower seismic sections. White rectangle shows the location of (b) map showing lineaments. Lower figures show (c) east and (d) west profiles from the north end of Budd Inlet, with sag feature and transparent zone that we interpret as faults (black vertical lines).

displacement suggest strike-slip motion. The dipping reflectors project across the deformed zone with little, if any, net vertical motion.

Discussion

Tacoma Fault Zone

Our results from Case Inlet suggest that the lineaments apparent on the LiDAR data in the western Tacoma fault zone are fold scarps rather than surface ruptures. This hypothesis means that trenches across the lineaments will exhume only minor, secondary faults accommodating the folding, as seems to be the case with the Catfish Lake fold scarp described here. Interpretation of past events rests in part on interpreting the fold growth through dating of growth strata. A combination of shallow seismic reflection data to define the fold geometry and coring to obtain samples for dating the growth strata on folds was used successfully to obtain ages of past events on growth folds in the Puente Hills fault zone in Los Angeles (Pratt *et al.*, 2002; Dolan *et al.*, 2003; Leon *et al.*, 2007). These same methods of growth analysis presumably could be applied in the Puget Lowland region.

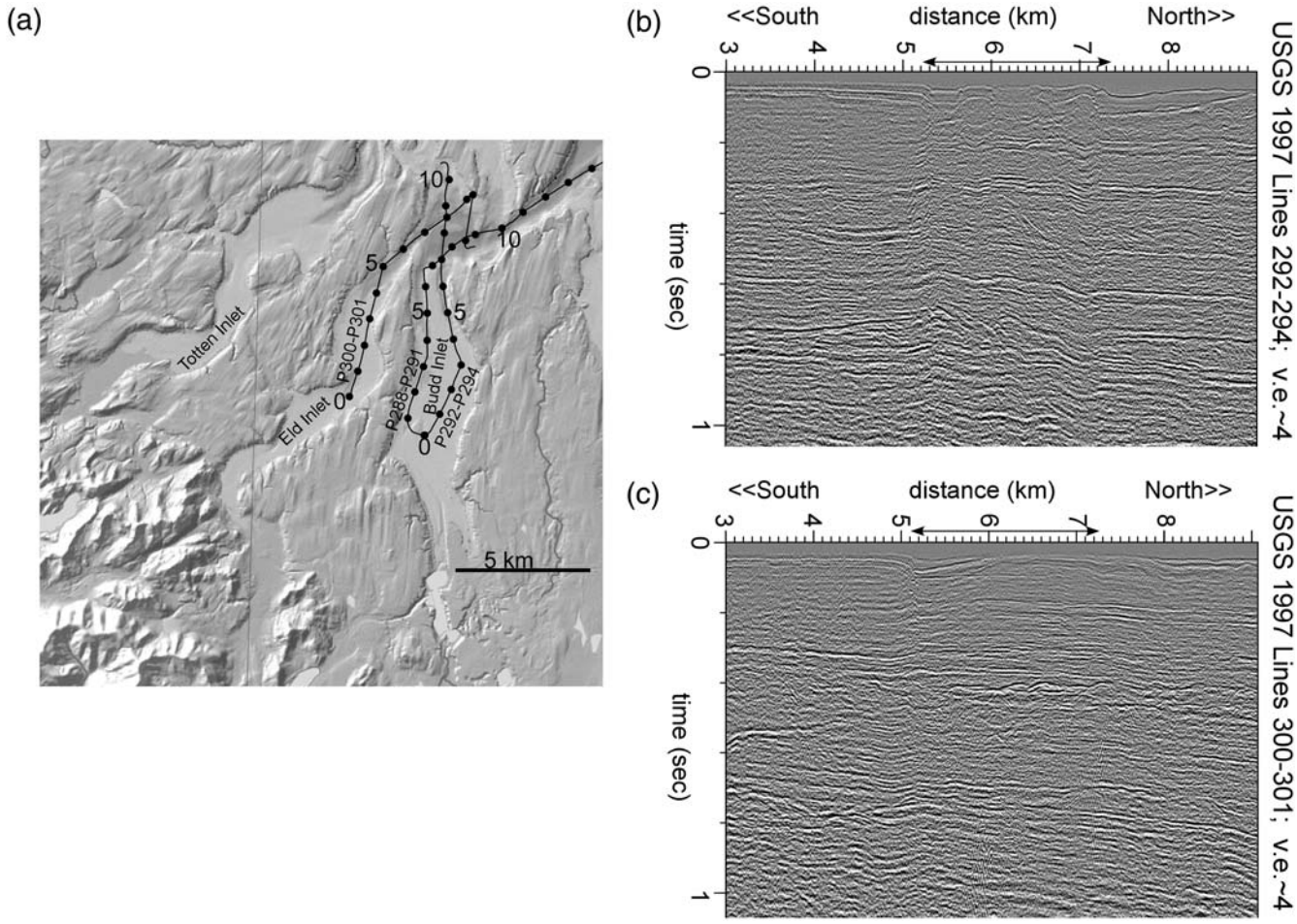

Figure 7. Unpublished seismic reflection profiles from the surveys of Johnson *et al.* (2004) showing a 2-km wide zone of shallow folding and faulting near the north ends of Budd and Eld Inlets. (a) Numbered track lines with black dots at 1-km intervals. (b,c) Data along track lines 292–294 and 300–301. The gently north-dipping reflectors on the profiles show a distinct zone of deformation between distances 5 and 7.5 km (black arrows at tops of sections) that includes folding and possibly small displacements from faulting. The distinct step in the water bottom overlying the fold or fault just north of the 5 km distance marks appears to be common to all of the profiles in the area. If they are part of a single feature, it has a northwest trend.

We propose that the kink band we imaged in Case Inlet formed in the Quaternary above a steeply dipping reverse or oblique-slip fault (Fig. 3d). The vertical displacement across this kink band on the deeper Quaternary layers is relatively small (Johnson *et al.*, 2004). The amount of pre-Quaternary displacement on the fault is unknown, but potential field data (Fig. 1; Pratt *et al.*, 1997), tomographic data (Brocher *et al.*, 2001), and its location at the north edge of the Tacoma basin suggest it is part of a fault system with kilometers of displacement. We cannot determine amounts of strike-slip motion, if any, except that it is too small to be obvious in the late Pleistocene to Holocene surface features.

Recent uplift in the last earthquake, as denoted by the change in depth of the water bottom, is concentrated in the central or north central part of the kink band. Johnson *et al.* (2004) interpret the kink band as an upward-narrowing growth triangle. However, the seismic profiles seem to show a fanning of reflector dips similar to those expected in progressive limb rotation (e.g., Hardy and Poblet, 1994). The narrower uplift of the water bottom suggests that the kink band is the sum of a number of narrower folds. The kink band thus appears to have grown in discreet increments both vertically and horizontally.

Within the central Tacoma fault zone, the faults we imaged demonstrate postglacial motion at the south edge of the Seattle uplift. Such motion was known in the west part of the Tacoma fault because of the Catfish Lake fold scarp and the land-level changes documented previously (Bucknam *et al.*, 1992; Sherrod *et al.*, 2004). In the case of the fault we imaged beneath central Carr Inlet, the latest deformation has a sense of motion opposite to the long-term motion (Fig. 5b), requiring a backthrust if the fault is part of a deep structure. A likely alternative is that we imaged small faults associated with bending at the synclinal axial surface at the base of the Rosedale monocline. In this interpretation, the faults would have little displacement and would sole into bedding planes at shallow depths. Such faults could be very limited in their lateral extent and could have opposite senses

of displacement. Another alternative is that the faults in the central Tacoma fault zone beneath Carr Inlet may be part of the broader deformation zone. One possibility is that a deep thrust or reverse fault below the synclinal axial surface ruptures in major earthquakes, with most of the deformation being consumed by folding and only a small part of the motion reaching the surface as faults. These small faults distribute the deformation over a broad zone and are not visible on deeper seismic reflection profiles (Pratt *et al.*, 1997) because their displacement is less than the resolution of the data. A final alternative is that the Rosedale monocline and the faults are responses to two different stresses: the fold forming in response to thrusting and the faults being caused by strike-slip motion parallel to the axial surfaces of the monocline.

The fault-like structures we imaged beneath Carr Inlet are unlikely to be caused by landslides. Some lie near the center of the broad inlet with little relief on the water bottom, and far enough from the shoreline to be beyond the toe of even deep-seated landslides. More problematic is the possibility that the shallow faults are due to compaction or settling, because the area was covered by ice during the last glaciation. A tectonic origin is consistent with their location above a large fold (the Rosedale monocline) that may be associated with deep, active faults in the region (Pratt *et al.*, 1997; Johnson *et al.*, 2004).

The presence of the faults and folds in areas where the gas-saturated layers are missing in Carr and Case Inlets suggests a relationship between the faults and the gas deposits. Deformation associated with the faults and folds may have released or prohibited the formation of gas accumulations, leaving windows of signal penetration along the faults. This implies that the distribution of windows through the gas layers could be used to identify areas of recent faulting throughout southern Puget Sound.

Olympia Structure

Our study documented the presence of active faults within the broader Olympia structure beneath the southern end of the Puget Lowland. Whether the faults we imaged are at the tip of a major fault zone or are small bending-moment faults within a fold, they require late Pleistocene to Holocene motion on faults either within or beneath the structure. Active faults are consistent with the large geophysical anomalies and the land-level changes along the Olympia structure (Gower *et al.*, 1985; Finn, 1990; Finn *et al.*, 1991; Bucknam *et al.*, 1992; Sherrod, 2001).

The faulted, subhorizontal beds that we imaged are likely postglacial strata filling a channel, which implies late Pleistocene or Holocene faulting. The 10 to 30 m of burial for the reflector sequence requires a Holocene age if we assume the average deposition rate in southern Puget Sound of 0.5–3.5 cm/yr (Carpenter *et al.*, 1985; Lavelle *et al.*, 1986). However, all of the subhorizontal strata we imaged may have been deposited very soon after the late Pleistocene glaciation, when the deposition rate was likely much higher than now. The faults have possibly been active since the Miocene or Oligocene, as the 3.5 to 6 km of vertical change in the elevation of the Crescent Formation between the Black Hills and the Tacoma basin suggests long-term motion similar to that on the major fault zones to the north (e.g., Johnson *et al.*, 1994; Pratt *et al.*, 1997; ten Brink *et al.*, 2002). The industry seismic reflection profiles do not extend far enough to the south to see whether deeper strata are broken by faults (Pratt *et al.*, 1997).

We interpret the apparent faults beneath Budd Inlet as having a tectonic origin rather than being deformation caused by compaction during glaciation or glacial rebound. The main arguments for a tectonic origin are the differing senses of displacement on reflectors at different depths (Fig. 6c), their location above a deformed area within the deeper strata, and the coincidence of the apparent faults with a major tectonic feature defined by the southern edge of the Tacoma basin and potential field anomalies. Glacial features would produce shallow faults in which all strata show the same sense of displacement. Also, if our interpretation of the stratigraphy is correct, the subhorizontal strata are recessional deposits that have not been compressed by glacial ice. Glacial deformation also would not be expected to extend into the older, deeper strata as we see on the deeper seismic profiles. A second possibility is a deep-seated slide feature, but the lack of steep topography perpendicular to the trend of the sag feature argues against a slump or landslide.

The lack of a thrust fault on the deeper data indicates that the shallow faults found in our surveys are likely part of a strike-slip fault zone. The gentle folding and faults with little apparent vertical displacement in the deeper strata are consistent with strike-slip faults, but the subdued deformation we imaged suggests a relatively small total displacement. Alternatively, the faults are shallowly rooted, bending-moment faults accommodating folding in the underlying strata. The latter explanation would be consistent with the interpretation of Pratt *et al.* (1997), including a slight change in dip angle (~2° to 4°) of basin strata at the south end of the Tacoma basin.

If the shallow faults beneath northern Budd Inlet are related to a major structure, they are likely splays that lie north of the fault that has the largest displacement of basement rocks. A pronounced gravity gradient spans the length of the inlet (Finn *et al.*, 1991), and the abrupt change in magnetic anomalies from low frequency in the northeast to high frequency in the southwest occurs beneath the central or southern part of Budd Inlet, several kilometers south of the shallow faults (Fig. 1). If these potential field anomalies are related to a major fault in the basement rocks, as seems likely, the faults we imaged beneath northern Budd Inlet lie several kilometers north of this major basement structure.

The locations of our profiles in Budd Inlet are south of the industry seismic profiles in Puget Sound, the southernmost of which shows a strong, north-sloping reflector that was interpreted as the top of Crescent Formation (Pratt *et al.*, 1997). This reflector lies at slightly more than 1 km depth at

the south end of the industry profile, about 2 km north of the faults we imaged. Based on the slope seen on the industry data, the basement reflector probably lies at about 800 m depth beneath the faults we imaged, and at about 200 m depth beneath the south end of the inlet. However, the sloping reflector projects to sea level at a location where basement rocks lie at an elevation of about 200 m in the Black Hills south of Budd Inlet, which suggests that a fault or fold with at least 200 m of vertical change could lie beneath southern Budd Inlet. A logical interpretation is that we are imaging a splay fault that lies several kilometers northeast of a thrust fault that lifts Crescent Formation rocks to the surface in the Black Hills. We do not see obvious deformation at the location of the main fault, but there is little or no signal penetration in our other profiles across the structure.

Conclusions

In the western Tacoma fault zone, our shallow seismic data show distinct growth strata above a narrow (360-m wide) kink band visible in deeper strata on previously published data. Onlapping of postglacial strata onto older surfaces, apparent warping of the water bottom, correlation with scarps, and an uplifted marine terrace north of the kink band are consistent with a large earthquake about 1100 years ago. The growth folding within the kink band demonstrates motion in the Quaternary, although older strata at depths of about 300 m do not appear to show growth folding.

Within the central Tacoma fault zone, our seismic reflection profiles show shallow, postglacial faults above the Rosedale monocline. We interpret one fault with south side up motion to cut postglacial strata just south of the monocline; other faults that appear to cut pre-Vashon glacial deposits and warp postglacial strata lie near the synclinal axis of the monocline. The relationship between these faults and the monocline visible on deeper data is unknown, but they may be small faults cutting through the monocline or bending-moment faults formed in response to continued growth of the monocline.

Our high-resolution seismic reflection surveys document late Pleistocene to Holocene faults within the Olympia structure. Two sag features are visible on seismic profiles from both sides of Budd Inlet. These features align with weak lineaments visible nearby in LiDAR data, although these lineaments are not clearly identifiable as scarps. A second fault is imaged about 160 m north of the sag feature. These faults overlie an ~ 2-km wide deformed zone visible on deeper seismic data. The lineaments and the likely postglacial age of the strata visible on the seismic profiles suggest late Pleistocene or Holocene motion along the fault. Although the shallow strata are displaced down to the north, strike-slip motion also is suggested from the seismic profiles because of the opposite sense of displacement seen on reflectors at different depths, the near-vertical attitude of the faults, and the relatively small vertical displacements of older strata. In either case, documentation of faults cutting the late Pleistocene to Holocene strata indicates the structure poses an earthquake hazard.

Data and Resources

The airgun data of Johnson *et al.* (2004) are available on the USGS Coastal and Marine website: http://walrus.wr.usgs.gov/infobank/g/g297ps/html/g-2-97-ps.meta.html (last accessed 1 April 2010).

The sparker seismic data we collected for this article are available at the Incorporated Research Institutes for Seismology Data Management System as an assembled data set named SOUTHPUGET. The data are in SEG-Y format and arranged in directories named for the students who collected the data (Crouch, Clement). Within the directories are postscript images of the data and Excel spreadsheets containing the navigation data.

Acknowledgments

John Crouch was instrumental in acquiring and helping to analyze the Tacoma fault portions of the data. Funding for this project was provided by the School of Oceanography, University of Washington, as part of senior research projects by John Crouch and Curtis Clement. Dave Thoreson operated the R/V *WeeLander* under challenging weather and sea conditions, and Floyd McCroskey kept equipment maintained and ready for use. Dick Sylwester of Northwest Geophysical Services provided some of the seismic system components. LiDAR data were provided courtesy of the Puget Sound LiDAR Consortium. Magnetic data were provided by R. Blakely of the U.S. Geological Survey. We thank Derek Booth, Ralph Haugerud, Robert Karlin, Harvey Kelsey, Mark Hemphill-Haley, and an anonymous reviewer for their suggestions for improving the article.

References

Blakely, R. J., R. E. Wells, and C. S. Weaver (1999). Puget Sound aeromagnetic maps and data, *U.S. Geol. Surv. Open-File Rept. 99-514*, http://pubs.usgs.gov/of/1999/of99-514/.

Blakely, R. J., R. E. Wells, C. S. Weaver, and S. Y. Johnson (2002). Location, structure, and seismicity of the Seattle fault zone, Washington: Evidence from aeromagnetic anomalies, geologic mapping, and seismic-reflection data, *Geol. Soc. Am. Bull.* **114,** 169–177.

Booth, D. B. (1994). Glaciofluvial infilling and scour of the Puget Lowland, Washington, during ice-sheet glaciation, *Geology* **22,** 695–698.

Booth, D. B., K. G. Troost, J. J. Clague, and R. B. Waitt (2004). The Cordilleran Ice Sheet: Chapter 2, in A. Gillespie, S. C. Porter, and B. Atwater (Editors), *The Quaternary Period in the United States*, International Union for Quaternary Research, Elsevier Press, pp. 17–43.

Brocher, T. M., R. J. Blakely, and R. E. Wells (2004). Interpretation of the Seattle Uplift, Washington, as a passive roof duplex, *Bull. Seismol. Soc. Am.* **94,** 1379–1401.

Brocher, T. M., T. Parsons, R. J. Blakely, N. I. Christensen, M. A. Fisher, R. E. Wells , and The SHIPS working group (2001). Upper crustal structure in Puget Lowland, Washington: Results from the 1998 Seismic Hazards Investigation on Puget Sound, *J. Geophys. Res.* **106,** 13,541–13,564.

Bucknam, R. C., E. Hemphill-Haley, and E. B. Leopold (1992). Abrupt uplift within the past 1700 years at southern Puget Sound, Washington, *Science* **258,** 1611–1614.

Carpenter, R., M. L. Peterson, and J. T. Bennett (1985). P^{210}b-derived sediment accumulation and mixing rates for the greater Puget Sound region, *Mar. Geol.* **64,** 291–312.

Dolan, J. F., S. A. Christofferson, and J. H. Shaw (2003), Recognition of paleoearthquakes on the Puente Hills blind thrust fault, California, *Science* **300,** 115–118, doi 10.1126/science.1080593.

Finn, C. (1990). Geophysical constraints on Washington convergent margin, *J. Geophys. Res.* **95,** pp. 19,533–19,546.

Finn, C., W. M. Phillips, and D. L. Williams (1991). Gravity anomaly and terrain maps of Washington, *U.S. Geol. Surv. Geophys. Invest. Map GP-988*.

Gower, H. D., J. C. Yount, and R. S. Crosson (1985). Seismotectonic map of the Puget Sound region, Washington, *U.S. Geol. Surv. Misc. Invest. Ser. Map I-1613*.

Hardy, S., and J. Poblet (1994). Geometric and numerical model of progressive limb rotation in detachment folds, *Geology* **22,** 371–374.

Haugerud, R. A., D. J. Harding, S. Y. Johnson, J. Harless, C. S. Weaver, and B. L. Sherrod (2003). High-resolution LiDAR topography of the Puget Lowland, Washington—A bonanza for earth science, *GSA Today* **13,** no. 6, 4–10.

Johnson, S. Y., R. J. Blakely, W. J. Stephenson, S. V. Dadisman, and M. A. Fisher (2004). Active shortening of the Cascadia forearc and implications for seismic hazards of the Puget Lowland, *Tectonics* **23,** TC1011, doi 10.1029/2003TC001507.

Johnson, S.Y., C. J. Potter, and J. M. Armentrout (1994). Origin and evolution of the Seattle fault and Seattle basin, Washington, *Geology* **22,** 71–74.

Kelsey, H. M., B. L. Sherrod, A. R. Nelson, and T. M. Brocher (2008). Earthquakes generated from bedding plane-parallel reverse faults above an active wedge thrust, Seattle fault zone, *Geol. Soc. Am. Bull.* **120,** 1581–1597, doi 10.1130/B26282.1.

Lavelle, J. W., G. J. Massoth, and E. A. Crecelius (1986). Accumulation rates of recent sediments in Puget Sound, Washington, *Mar. Geol.* **72,** 59–70.

Leon, L. A., S. A. Christofferson, J. F. Dolan, J. H. Shaw, and T. L. Pratt (2007). Earthquake-by-earthquake fold growth above the Puente Hills blind thrust fault, Los Angeles, California: Implications for fold kinematics and seismic hazard, *J. Geophys. Res.* **112,** B03S03, doi 10.1029/2006JB004461.

Liberty, L. M., and T. L. Pratt (2008). Structure of the eastern Seattle fault zone, Washington State: New insights from seismic reflection data, *Bull. Seismol. Soc. Am.* **98,** no. 4, 1681–1695, doi 10.1785/0120070145.

Nelson, A. R., S. Y. Johnson, H. M. Kelsey, R. E. Wells, B. L. Sherrod, S. K. Pezzopane, L. A. Bradley, R. D. Koehler, and R. C. Bucknam (2003). Late Holocene earthquakes on the Toe Jam Hill fault, Seattle fault zone, Bainbridge Island, Washington, *Geol. Soc. Am. Bull.* **115,** no. 11, 1388–1403.

Palmer, S. P., T. J. Walsh, and W. J. Gerstel (1999). Geologic Folio of the Olympia-Lacey-Tumwater Urban area, Washington: Liquefaction Susceptibility Map, Washington State Department of Natural Resources Geologic Map GM-47.

Porter, S. C., and T. W. Swanson (1998). Radiocarbon age constraints on rates of advance and retreat of the Puget lobe of the Cordilleran ice sheet during the last glaciation, *Quaternary Res.* **50,** 205–213.

Pratt, T. L., M. Holmes, E. S. Schweig, J. Gomberg, and H. A. Cowan (2003). High resolution seismic imaging of faults beneath Limón Bay, northern Panama Canal, Republic of Panama, *Tectonophysics* **368,** 211–227.

Pratt, T. L., S. Johnson, C. Potter, W. Stephenson, and C. Finn (1997). Seismic reflection images beneath Puget Sound, western Washington State: The Puget Lowland thrust sheet hypothesis, *J. Geophys. Res.* **102,** 27,469–27,489.

Pratt, T. L., J. Odum, W. Stephenson, R. Williams, S. Dadisman, M. Holmes, and B. Haug (2001). Late Pleistocene and Holocene tectonics of the Portland Basin, Oregon and Washington, from high-resolution seismic profiling, *Bull. Seismol. Soc. Am.* **91,** 637–650.

Pratt, T. L., J. H. Shaw, J. F. Dolan, S. Christofferson, R. A. Williams, J. K. Odum, and A. Plesch (2002). Shallow seismic imaging of folds above the Puente Hills blind-thrust fault, Los Angeles, California, *Geophys. Res. Lett.* **29,** 18-1–18-4.

Sherrod, B. L. (2001). Evidence for earthquake-induced subsidence about 1100 yr ago in coastal marshes of southern Puget Sound, Washington, *Geol. Soc. Am. Bull.* **113,** 1299–1311.

Sherrod, B. L., R. J. Blakely, C. S. Weaver, H. M. Kelsey, E. Barnett, L. M. Liberty, K. L. Meagher, and K. M. Pape (2008). Finding concealed active faults: Extending the southern Whidbey Island fault across the Puget lowland, Washington, *J. Geophys. Res.* **113,** B05313, doi 10.1029/2007JB005060.

Sherrod, B. L., T. M. Brocher, C. S. Weaver, R. C. Bucknam, R. J. Blakely, H. M. Kelsey, A. R. Nelson, and R. Haugerud (2004). Holocene fault scarps near Tacoma, Washington, USA, *Geology* **32,** 9–12.

Sherrod, B. L., R. C. Bucknam, and E. B. Leopold (2000). Holocene relative sea level changes along the Seattle Fault at Restoration Point, Washington, *Quatenary Res.* **54,** 384–393.

Sherrod, B. L., A. Nelson, H. Kelsey, T. Brocher, R. Blakely, C. Weaver, N. Rountree, S. Rhea, and B. S. Jackson (2003). The Catfish Lake scarp, Allyn, Washington: Preliminary field data and implications for earthquake hazards posed by the Tacoma fault, *U.S. Geol. Surv. Open-File Rept. 03-455*.

ten Brink, U. S., P. C. Molzer, M. A. Fisher, R. J. Blakely, R. C. Bucknam, T. Parsons, R. S. Crosson, and K. C. Creager (2002). Subsurface geometry and evolution of the Seattle fault zone and Seattle Basin, Washington, *Bull. Seismol. Soc. Am.* **92,** 1737–1753.

Thorson, R. M. (1980). Ice-Sheet Glaciation of the Puget Lowland, Washington, during the Vashon Stade (late Pleistocene), *Quatenary Res.* **13,** 303–321.

U.S. Geological Survey, http://walrus.wr.usgs.gov/infobank/g/g297ps/html/g-2-97-ps.meta.html (last accessed 1 April 2010).

Van Wagoner, T. M., R. S. Crosson, K. C. Creager, G. Medema, L. Preston, N. P. Symons, and T. M. Brocher (2002). Crustal structure and relocated earthquakes in the Puget Lowland, Washington from high resolution seismic tomography, *J. Geophys. Res.* **107,** no. B12, ESE 22-1 to ESE 22-23, doi 10.10129/2001JB000710.

Wells, R., C. Weaver, and R. Blakely (1998). Fore-arc migration in Cascadia and its neotectonic significance, *Geology* **26,** 759–762.

School of Oceanography
Box 357940
University of Washington
Seattle, Washington 98195-7940
(C.R.C., M.L.H.)

U.S. Geological Survey
School of Oceanography, Box 357940
University of Washington
Seattle, Washington 98195-7940
(T.L.P.)

U.S. Geological Survey
Department of Earth and Space Sciences, Box 351310
University of Washington
Seattle, Washington 98195-1310
(B.L.S.)

Manuscript received 27 February 2007